Electronic Supplementary Material (ESI) for Dalton Transactions

A novel structural form of MIL-53 observed for the scandium analogue and its response to temperature variation and CO_2 adsorption

John P. S. Mowat,[a] Valerie R. Seymour,[a] John M. Griffin,[a] Stephen P. Thompson,[b] Alexandra M. Z. Slawin,[a] David Fairen-Jimenez,[c] Tina Düren,[c] Sharon E. Ashbrook [a] and Paul A. Wright*[a]

[a] *EASTCHEM School of Chemistry, University of St. Andrews, Purdie Building, North Haugh, St. Andrews, Fife, KY16 9ST, United Kingdom*

[b] *Diamond Light Source, Harwell Science and Innovation Campus, Didcot, Oxfordshire OX11 0DE, United Kingdom*

[c] *Institute for Materials and Processes, School of Engineering, The University of Edinburgh, United Kingdom*

Supporting Information

S1. Structural data for MIL-53(Sc)

S1.1 Single crystal X-ray diffraction details for MIL-53(Sc)-cp

Table S1.1.1 Crystallographic details for MIL-53(Sc)-*cp* from SXRD

S1.2 Variable temperature high resolution powder X-ray diffraction of MIL-53(Sc)

Fig S1.2.1 & S1.2.2 X-ray powder diffraction patterns for MIL-53(Sc) from 100 – 623 K

S1.3 Rietveld refinement details for MIL-53(Sc) from 100 K - 623 K.

Figure S1.3.1 Rietveld plot of refinement of MIL-53(Sc)-*cp* at 100 K.

Figure S1.3.2 Rietveld plot of refinement of MIL-53(Sc)-*cp* at 298 K.

Figure S1.3.3 Rietveld plot of refinement of MIL-53(Sc)-*vnp* at 623 K.

Table S1.3.1 Crystallographic data from the variable temperature series

S1.4 Thermogravimetric analysis of MIL-53(Sc)

Figure S1.4.1 TGA of desolvated MIL-53(Sc)

S2. Solid-state NMR on MIL-53(Sc)

S5. Computational Simulation of CO_2 Adsorption

S6. References

S1. Structural data for MIL-53(Sc)

S1.1 Single-crystal X-ray diffraction details for MIL-53(Sc)-cp

Single crystals of the MIL-53(Sc)-*cp* were prepared using the literature preparation.[1] A solution of scandium nitrate hydrate, terephthalic acid, pyridine and N,N-dimethylformamide in a molar ratio ($Sc(NO_3)_3{\cdot}3H_2O$):H_2BDC:C_5H_5N:DMF of 1:1:15:200 was stirred at room temperature and transferred to a Teflon lined stainless-steel autoclave and heated at 463 K for 40 hours. Samples were filtered, dried then heated under flowing nitrogen in a tube furnace at 623 K for 12 hours to ensure complete removal of solvent and any unreacted terephthalic acid. To ensure full de-solvation, a selection of the single crystals were transferred to a Schlenk tube and heated for 12 hours at 473 K *in vacuo* before the tube was backfilled with dry nitrogen. The crystals were kept under N_2 until single-crystal diffractometer time was available and the crystals were treated as air sensitive, minimizing exposure to air and therefore moisture that could affect the pore opening. The crystals were transferred directly to a poly-fluorinated oil for mounting on the diffractometer.

Single crystal diffraction data for dehydrated MIL-53(Sc) were collected at 293 K using a Rigaku MM007 High brilliance RA generator (Mo K_α radiation, confocal optics) and a Mercury CCD system. At least a full hemisphere of data was collected using ω scans. Intensities were corrected for the Lorentz-polarisation factor and for absorption. The structures were solved by direct methods and structural refinements were performed with full-matrix least-squares based on F^2 by using the program SHELXTL.[2]

Although the single crystal data were not of sufficient quality for structure refinement, it was possible to arrive at a unit cell and space group and a partial structure, including scandium positions. This was then used as a starting model for refinement of the structure against synchrotron X-ray powder diffraction patterns.

Table S1.1.1: Crystallographic details for MIL-53(Sc)-*cp* from single crystal diffraction

	MIL-53(Sc)-*cp*
Formula Unit	$ScOH(C_8H_4O_4)$
Formula Weight	202.05
Temperature/K	293
Space Group	$P\ 2_1/c$
X-ray Source	Mo K_α
Wavelength/Å	0.71075
Unit Cell: *a*/Å	20.37(2)
b/Å	7.357(8)
c/Å	11.605(14)
β/°	105.00(3)
Volume/ $Å^3$	1680(3)
Z	4
R	0.3872
wR	0.6437
Max and min residual e- density (e/$Å^3$)	1.992, -1.683

S1.2 High resolution and variable temperature powder X-ray diffraction on MIL-53(Sc)

Synchrotron X-ray diffraction data were obtained at the high resolution powder diffraction beamline I11 at the Diamond Light Source. Samples of the MIL-53(Sc) were synthesized as large single-crystals that were first ground to a fine powder to avoid preferential orientation and loaded into a quartz glass capillary. The sample was then heated under vacuum at 473 K for 12 hours and flame sealed to ensure the thermal behaviour was independent of adsorbed guest species. Data was collected between 100 K and 623 K, the temperature was controlled by means of a Cryostream 700 Series between 100 K and 293 K and using a hot air blower in the region above room temperature 293 K – 523 K. In each case the diffraction pattern was collected from 0-140° 2θ by constant velocity scanning in Debye -Scherrer geometry using the

multi-analyser crystal system available at beamline I11, with the measured intensities binned to a 2θ interval of 0.001°.

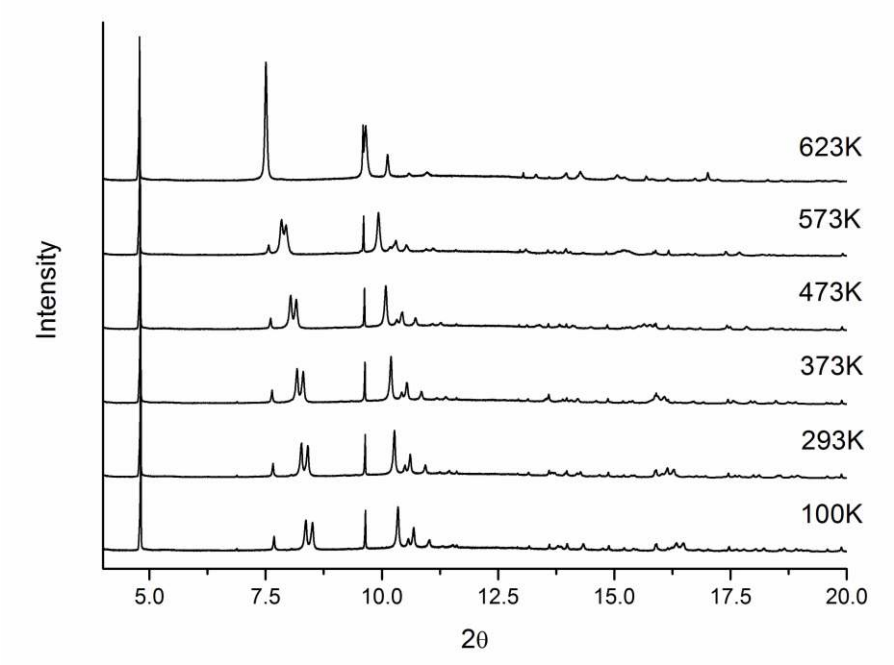

Figure S1.2.1 High resolution synchrotron X-ray powder diffraction patterns of dehydrated MIL-53(Sc) from 100 K to 623 K (λ = 0.825028 Å)

The patterns over the temperature range 100 – 573 K were indexed as monoclinic, *P* $2_1/c$, whereas at 623 K the pattern was indexed as *C* 2/*c*.

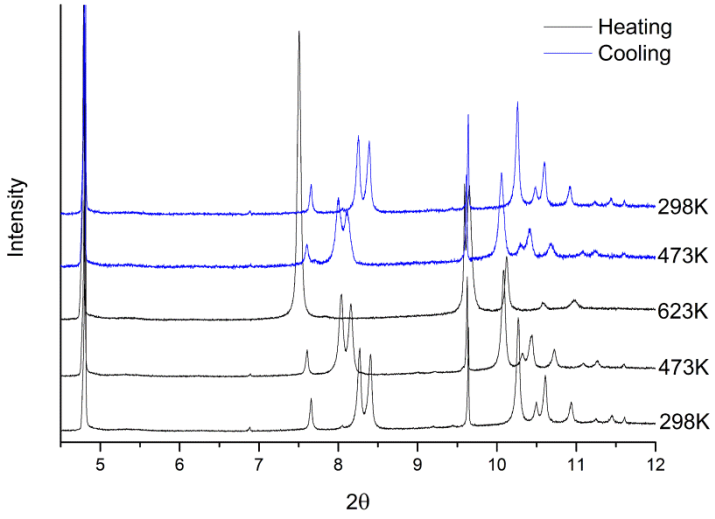

Figure S1.2.2 High resolution synchrotron X-ray powder diffraction patterns of dehydrated MIL-53(Sc) heating from 298 K to 623 K and cooling to 298K, showing the reversibility of the high temperature symmetry change. (λ = 0.825028 Å)

S1.3 Rietveld refinement details for MIL-53(Sc) from 100 - 623 K.

Rietveld refinement of the partial structure of dehydrated MIL-53(Sc) determined by single crystal diffraction and in the space group $P\ 2_1/c$ was performed to determine its structure over the temperature range 100 – 573 K. Two examples of the Rietveld profile fits are given below (Figures S1.3.1 and S1.3.2). At 623 K the structure has $C\ 2/c$ symmetry and the diffraction profile was fitted using the published structure of MIL-53(Fe)-*vnp* as a starting model for the refinement (Figure S1.3.3). The fit in all cases shows good agreement to the proposed models indicating that the bulk sample is at all temperatures well represented by the two structural models MIL-53(Sc)-*cp* and, at 623 K, MIL-53(Sc)-*vnp*.

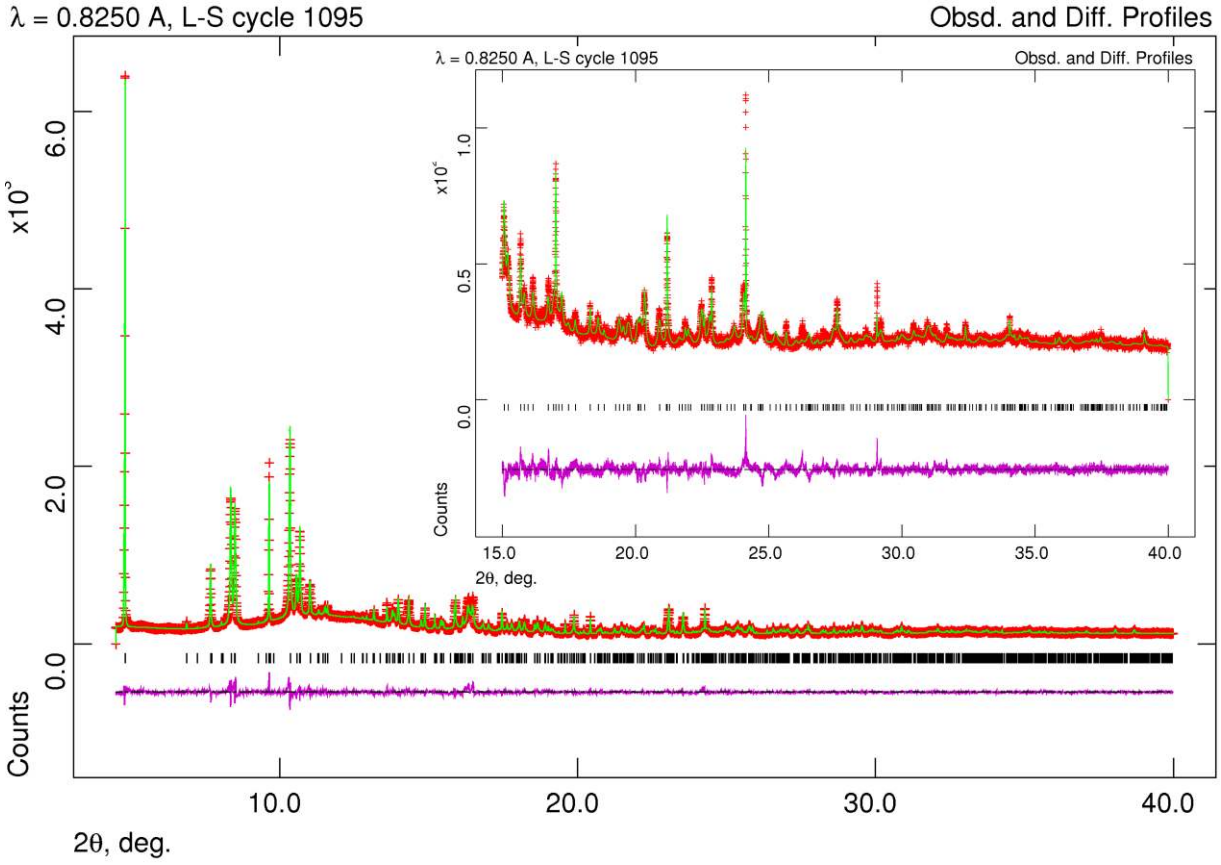

Figure S1.3.1 Rietveld profile fit to synchrotron diffraction data for MIL-53(Sc)-cp at 100 K. Red markers represent the experimental data; green line represents the fitted profile; purple line the difference plot. λ = 0.825028 Å, R_p = 0.0347, R_{wp} = 0.047.

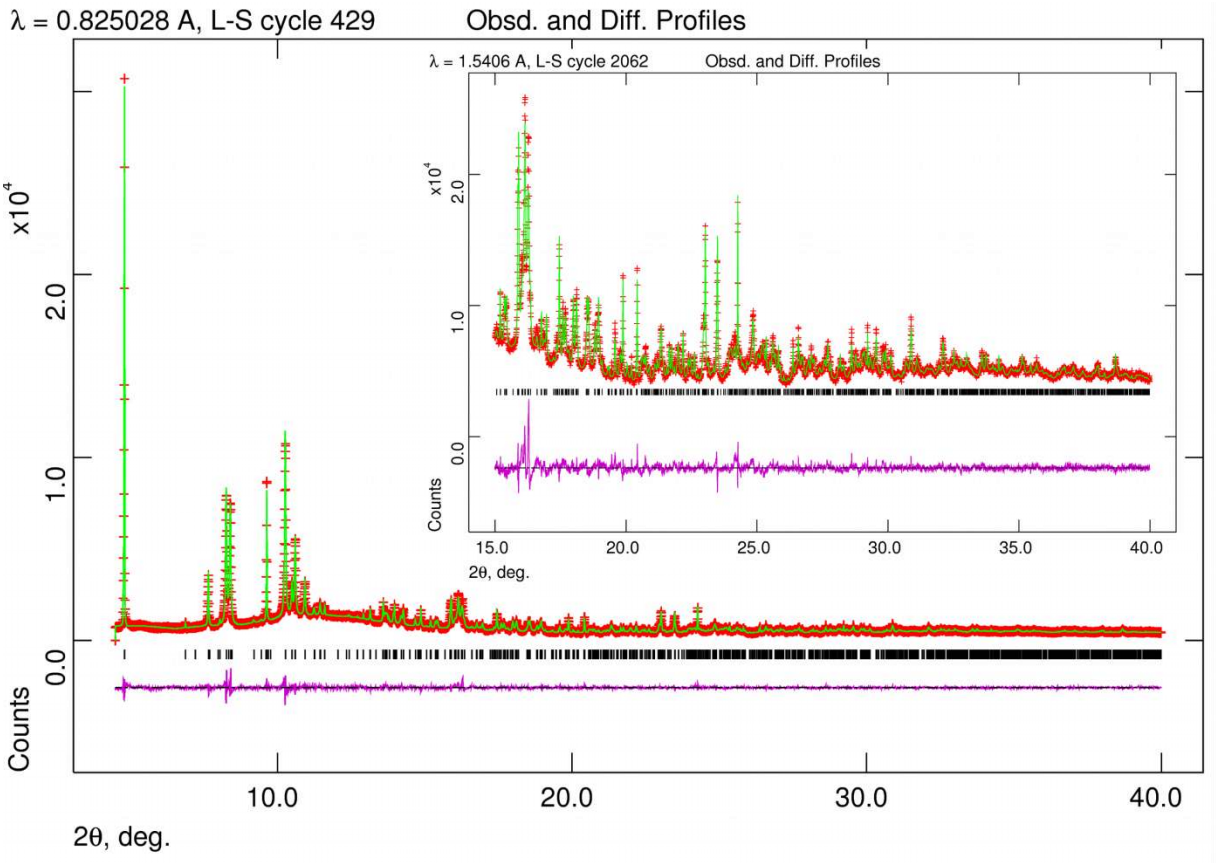

Figure S1.3.2 Rietveld profile fit to synchrotron diffraction data for MIL-53(Sc)-cp at room temperature (298 K). Red markers represent the experimental data; green line represents the fitted profile; purple line the difference plot. λ = 0.825028 Å, R_p = 0.0347, R_{wp} = 0.0449.

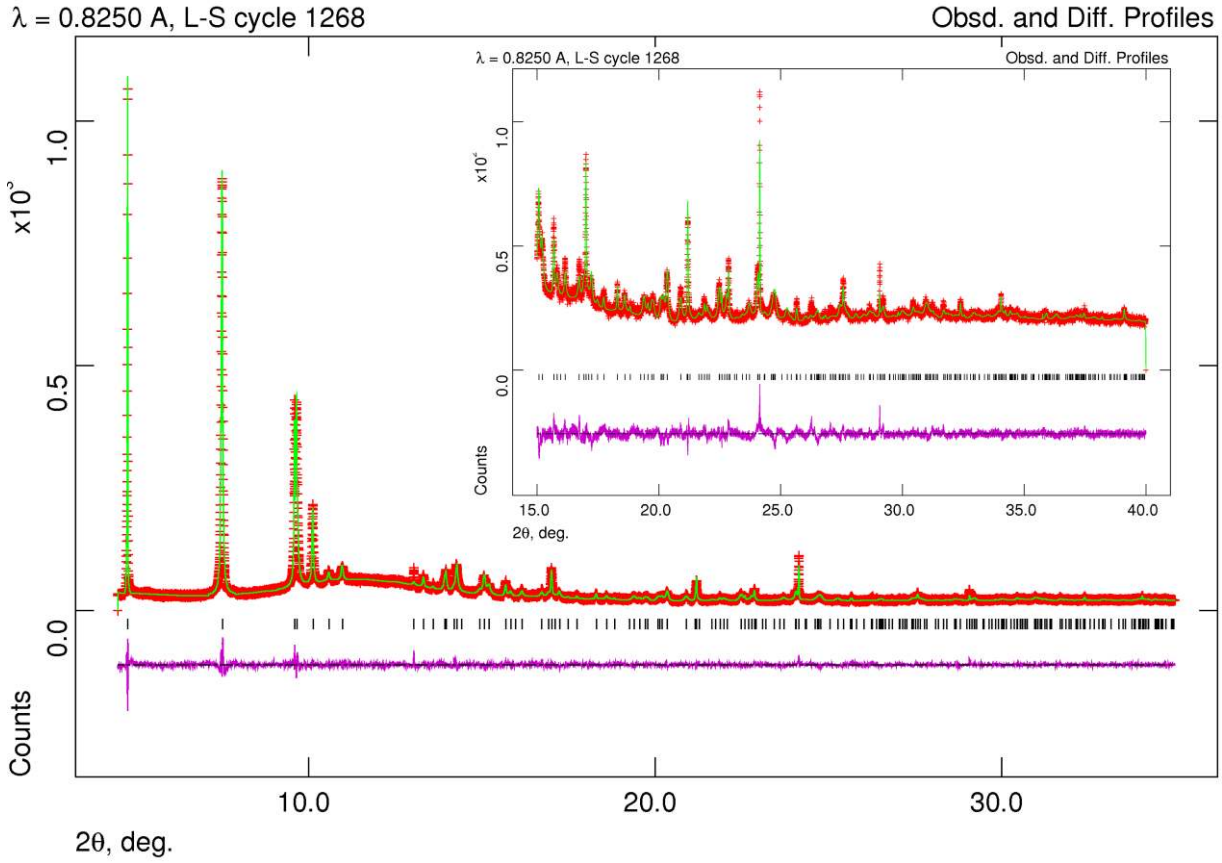

Figure S1.3.3 Rietveld profile fit to synchrotron diffraction data for MIL-53(Sc)-HT at 623 K. Red markers represent the experimental data; green line represents the fitted profile; purple line the difference plot. $\lambda =$ *0.825028 Å,* R_p *= 0.0409,* R_{wp} *= 0.538.*

Table S1.3.1 Crystallographic data from the variable temperature studies on MIL-53(Sc), obtained via Rietveld analysis of the synchrotron PXRD data obtained at the high resolution powder diffraction beamline I11 at the Diamond Light Source.

	100K	298 K	373K	473K	573K	623K
Formula Unit	$ScOH(C_8H_4O_4)$	$ScOH(C_8H_4O_4)$	$ScOH(C_8H_4O_4)$	$ScOH(C_8H_4O_4)$	$ScOH(C_8H_4O_4)$	$ScOH(C_8H_4O_4)$
Formula Weight	202.05	202.05	202.05	202.05	202.05	202.05
Temperature/K	100	293	373	473	573	623
Space Group	*P* $2_1/c$	*P* $2_1/c$	*P* $2_1/c$	*P* $2_1/c$	*P* $2_1/c$	*C* 2/*c*
X-ray Source	Synchrotron	Synchrotron	Synchrotron	Synchrotron	Synchrotron	Synchrotron
Wavelength/Å	0.825028	0.825028	0.825028	0.825028	0.825028	0.825028
Unit Cell: *a*/Å	20.29839(17)	20.3297(2)	20.36637(2)	20.4289(2)	20.53821(3)	21.5050(3)
b/Å	7.33083(8)	7.32576(8)	7.3192(9)	7.3117(1)	7.2992(1)	7.2743(2)
c/Å	11.6912(1)	11.8382(2)	11.9856(2)	12.2158(2)	12.5604(3)	6.63(8)
β/°	104.9584(12)	105.2058(12)	105.4664(12)	105.8726(14)	106.5514(17)	113.5427(15)
Volume/ $Å^3$	1680.75(3)	1701.36(3)	1721.95(4)	1755.14(4)	1804.95(5)	950.838(3)
Z	4	4	4	4	4	2
R_p	0.0347	0.0347	0.0338	0.034	0.0315	0.0409
R_{wp}	0.047	0.0449	0.0435	0.0439	0.0413	0.0538
Restraints	35	42	41	41	42	28
Max and min residual e- density (e/$Å^3$)	0.393, -0.488	0.263, -0.229	0.273, -0.307	0.419, -0.322	0.244, -0.245	0.578, -0.366

S1.4 Thermogravimetric analysis (TGA) of MIL-53(Sc)

To determine the thermal stability of MIL-53(Sc), TGA was performed at 5 K min^{-1} up to 1100 K in flowing air using a Netzsch TG 209 instrument on a sample pre-heated at 623 K for 12 hours in a tube furnace under flowing nitrogen.

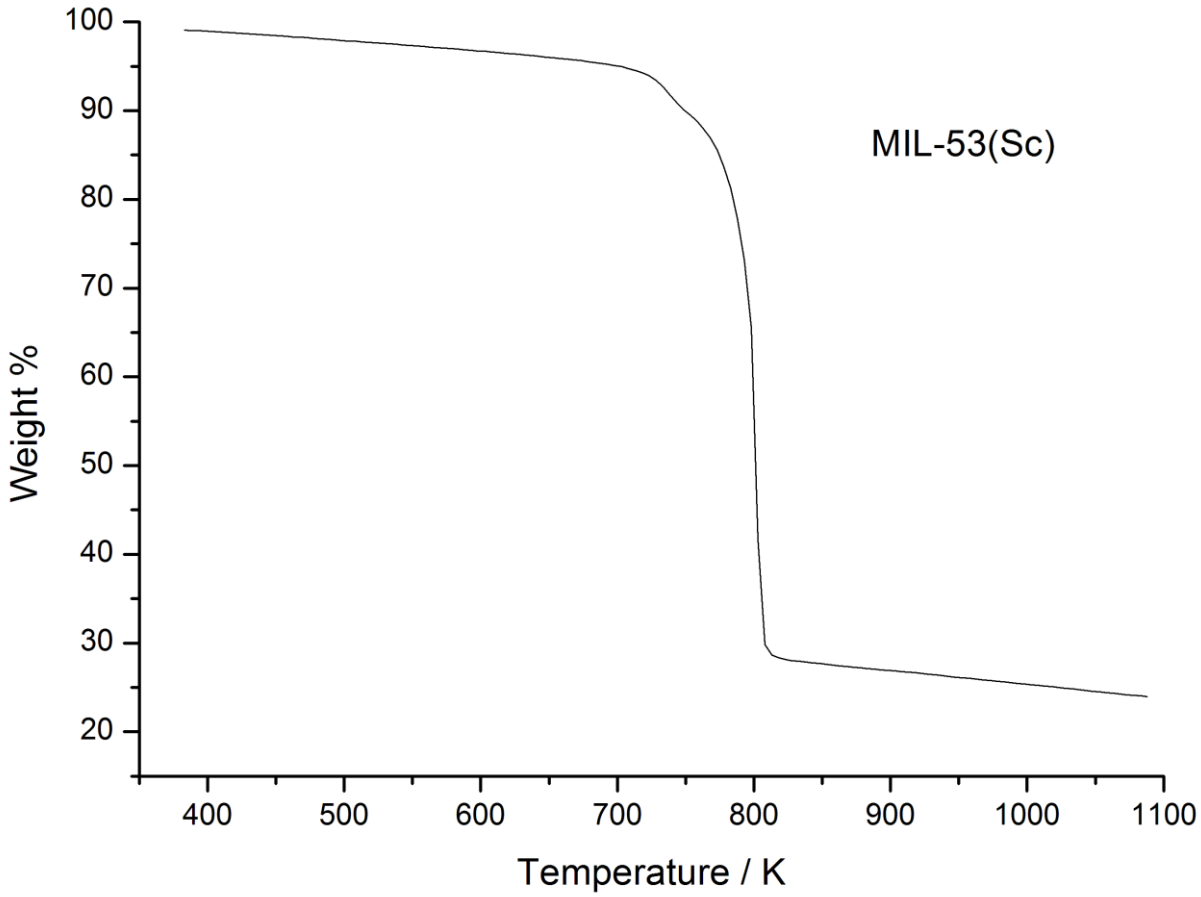

Figure S1.4.1 Thermogravimetric analysis of MIL-53(Sc) shows the material to be stable to heating up to temperatures >700 K under air. This is suitable for removal of unreacted linker molecules (terephthalic acid sublimes <623 K) and guest solvent molecules.

S2. Solid-state NMR

S2.1 Experimental and calculation details

^{13}C solid-state NMR experiments were performed using Bruker Avance III spectrometers operating at magnetic field strengths of 9.4 T or 14.1 T, with samples packed into 4-mm or 2.5-mm MAS rotors, respectively, and rotated at MAS rates of 12.5 kHz. ^{13}C transverse magnetisation was obtained by ramped cross polarisation (CP) from ^{1}H. Two-pulse phase modulation (TPPM) ^{1}H decoupling was applied during acquisition. For MIL-53(Sc), ^{45}Sc solid-state NMR experiments were performed using a Bruker Avance III spectrometer operating at a magnetic field strength of 20.0 T at the UK 850 MHz solid-state NMR facility. Spectra were acquired using a Bruker 2.5-mm probe at a MAS frequency of 30 kHz. ^{45}Sc triple-quantum MAS NMR spectra were recorded using a phase-modulated split-t_1 shifted-echo pulse sequence with the third pulse chosen to be selective for the central transition.[3] The indirect dimension is referenced as outlined in Ref.[4] For MIL-53(Sc)-NO_2, ^{45}Sc spectra were acquired using a Bruker Avance III spectrometer operating at a magnetic field strength of 14.1 T, and a Bruker 1.3-mm probe with a MAS frequency of 60 kHz. Variable-temperature ^{2}H NMR experiments were performed using a Bruker Avance III spectrometer operating at a magnetic field strength of 9.4 T. Spectra were acquired for a static sample using a Bruker 4-mm probe at temperatures of 298 and 373 K. A quadrupolar echo pulse sequence ($90°_{\varphi}$–τ–$90°_{\varphi'}$– τ) was used with an echo duration, τ, of 40 μs, together with a 16-step phase cycle designed to refocus both linear and quadratic spin interactions.[5] Chemical shifts are given relative to TMS for ^{13}C and ^{2}H and 0.2 M $ScCl_3$ (aq) for ^{45}Sc. Further experimental details are given in the figure captions.

DFT calculations were performed using CASTEP, a periodic planewave pseudopotential code[5] which utilizes the GIPAW formalism[6] to reconstruct the all-electron wave function in a magnetic field. The generalized gradient approximation (GGA) PBE functional was used and the core-valence interactions described by ultrasoft pseudopotentials. Integrals over the Brillouin zone were performed using a Monkhurst-Pack grid with a k-point spacing of 0.05 Å^{-1}. Wavefunctions were expanded in planewaves with a kinetic energy smaller than the cutoff energy, typically ~680 eV. Structural parameters (the unit cell and atomic positions) were obtained from diffraction data. Geometry optimization was also performed within CASTEP, with the unit cell size and shape remaining fixed. A quadrupole moment, eQ, of –220 mB, was used for ^{45}Sc.

S2.2 NMR, full structural characterisation details

To support the structures obtained from diffraction data, ^{45}Sc and ^{13}C solid-state MAS NMR experiments were performed on dehydrated and subsequently rehydrated MIL-53(Sc). For ^{13}C, the spectra in Figure S2.3.1 for dehydrated and rehydrated materials both show two main groups of peaks, corresponding to aromatic carbons (between 120 and 140 ppm) and carboxylate carbons (between 170 and 180 ppm). For dehydrated MIL-53(Sc) two clear peaks are observed in the carboxylate region (at δ = 172.5 and 176.9 ppm), along with a complex lineshape in the aromatic region.

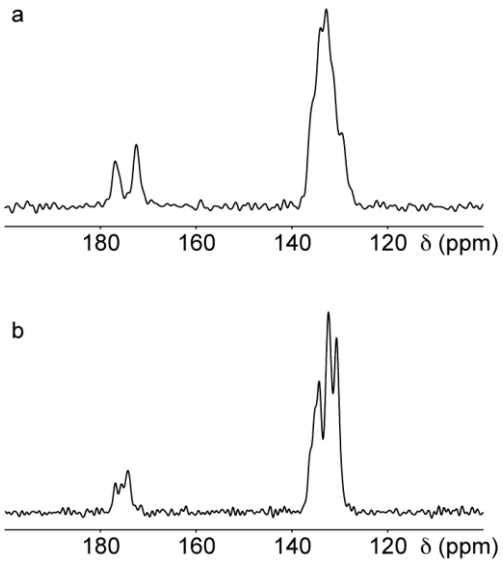

Figure S2.2.1 (^{13}C spectra): ^{13}C CP MAS NMR spectra of (a) dehydrated and (b) rehydrated MIL-53(Sc) recorded at a magnetic field strength of 14.1 T and a MAS rate of 12.5 kHz, using a 2.5-mm MAS probe. Spectra are the result of co-adding (a) 5120 and (b) 5784 transients separated by recycle intervals of 3 s, with a contact time of 1 ms.

For the rehydrated material, more ^{13}C resonances are observed in the carboxylate region, in agreement with the reduction in symmetry and the increased number of crystallographically-distinct species expected. The spectra shown here would suggest that

the ^{13}C MAS NMR spectrum of dehydrated MIL-53(Sc) shown in previous work[1] was not of a perfectly dehydrated material, but had some water incorporated within the pores.

^{45}Sc MAS NMR spectra (Figure S2.2.2) acquired at 20.0 T at the UK 850 MHz solid-state NMR facility. In each spectrum composite resonances corresponding to the overlap of quadrupolar-broadened powder-pattern lineshapes are observed, and the two spectra look very similar. In order to attempt to resolve the distinct species two-dimensional high-resolution multiple-quantum (MQ) MAS ^{45}Sc spectra were measured using a phase-modulated split-t_1 shifted-echo experiment.[4,5] The use of the high magnetic field strength will reduce the quadrupolar broadening (proportional to $1/B_0$), easing the implementation of the experiment, and may help to increase resolution of the distinct Sc species. For the dehydrated material, two ^{45}Sc sites are clearly resolved (at δ_1 values of 14.6 and 15.2 ppm), with quadrupolar products P_Q (= $C_Q(1 + \eta_Q^2/3)^{1/2}$) of 14.7 and 15.6 MHz and isotropic chemical shifts of ~55.1 and ~56.9 ppm, respectively. For the rehydrated MIL-53(Sc), two resonances are also observed (now at δ_1 values of 15.7 and 16.7 ppm), but their relative intensity ratios (1 : 3) are consistent with the presence of four ^{45}Sc species, three of which are coincident in d_1. It is difficult to extract accurate NMR parameters from this spectrum, owing to the overlap of the signals, but it is clear that generally the Sc species have higher C_Q values (16.5-16.8 MHz) and higher isotropic chemical shifts (57-62 ppm) than observed for dehydrated MIL-53(Sc).

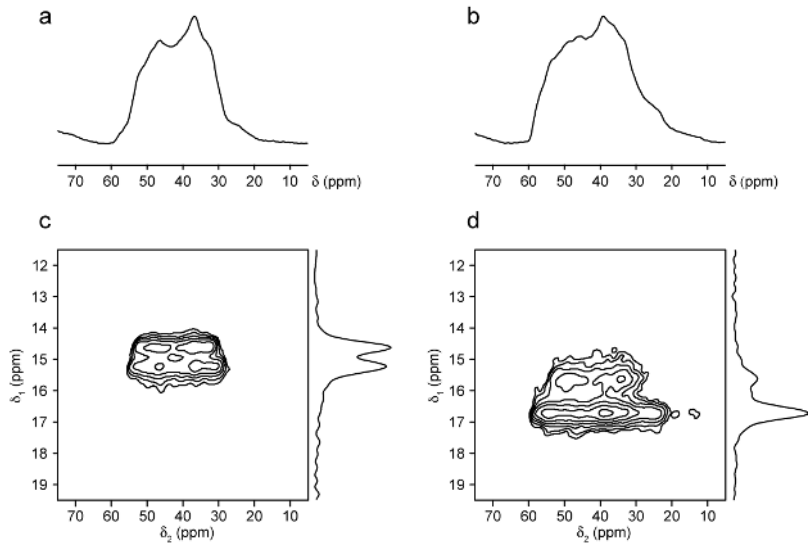

Fig.S2.2.2 *^{45}Sc NMR spectra of MIL-53(Sc) recorded at a magnetic field strength of 20.0 T and a MAS rate of 30 kHz, using a 2.5-mm MAS probe. Conventional MAS spectra of (a) dehydrated and (b) rehydrated samples are the result of co-adding 1024 transients*

separated by recycle intervals of (a) 3 and (b) 0.5 s. Two-dimensional triple-quantum MAS spectra of (c) dehydrated and (d) hydrated samples are the result of co-adding 192 transients separated by recycle intervals of (c) 2 s and (d) 0.5 s, for each of (c) 118 and (d) 124 t_1 increments of 108.15 ms.

To help interpret the MAS spectra, NMR parameters were calculated using the periodic planewave DFT code CASTEP.[6,7] The structures obtained from diffraction were geometry optimised (minimising the forces upon the atoms) with the atomic coordinates varied and the unit cell size and shape retained. This resulted in the phenyl groups becoming more planar and an improvement in the positioning of the H atoms, but the structures remained very similar. After optimization the NMR parameters for both the dehydrated and rehydrated structures were calculated. For the dehydrated material there is good agreement between experiment and calculation, with C_Q values for the two ^{45}Sc species of 15.2 (Sc1) and 14.1 MHz (Sc2) (and corresponding P_Q values of 15.9 and 14.7 MHz, respectively), although the difference in isotropic chemical shift between the two is slightly overestimated (~ 4 ppm cf 1 ppm).

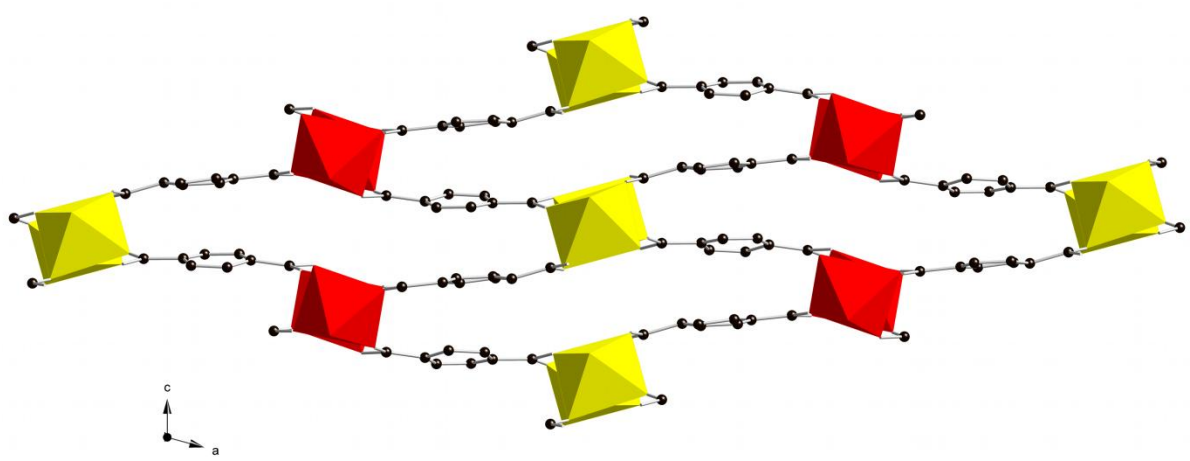

Figure S2.2.3 MIL-53(Sc) structure at 298K with the two crystallographically distinct sites Sc1 and Sc2 identified as red (ScO_6) and yellow (ScO_6) polyhedral respectively.

The agreement is sufficient to enable the two ^{45}Sc resonances in the experimental spectrum in Figure S2.3 to be assigned as Sc2 (δ_1 = 14.6 ppm) and Sc1 (δ_1 = 15.2 ppm). For the dehydrated material, the calculated parameters are in broad agreement with those determined experimentally, with C_Q values between 16.5 and 17.3 MHz (and P_Q values between 16.8 and 17.6 MHz), and generally higher isotropic chemical shifts. The

agreement between calculation and experiment for this rehydrated material is perhaps not expected to be as good as that observed for dehydrated MIL-53(Sc), owing to the presence of water molecules within the pores and, consequently, possible disorder and dynamics. For the ^{13}C NMR spectra, good agreement is also obtained between experiment and calculation for the resonances in the carboxylate region (those in the aromatic region are too overlapped for detailed analysis). For dehydrated MIL-53(Sc) four carboxyl species are expected, but the calculation shows these are present in two resonances (each containing two species), separated by ~5.3 ppm. In the rehydrated material eight resonances are predicted within ~4 ppm, again in good agreement with the experimental spectrum.

S2.3 Solid state wideline ^{2}H NMR of deuterated MIL-53(Sc)

^{2}H wideline NMR spectra recorded at temperatures of 298 and 373 K are shown in Figure S2.3.1. At both temperatures, the spectra are dominated by a characteristic Pake doublet powder lineshape, with a pair of singularities, or 'horns', separated by ~130 kHz, which is typical for aromatic CH deuterons.

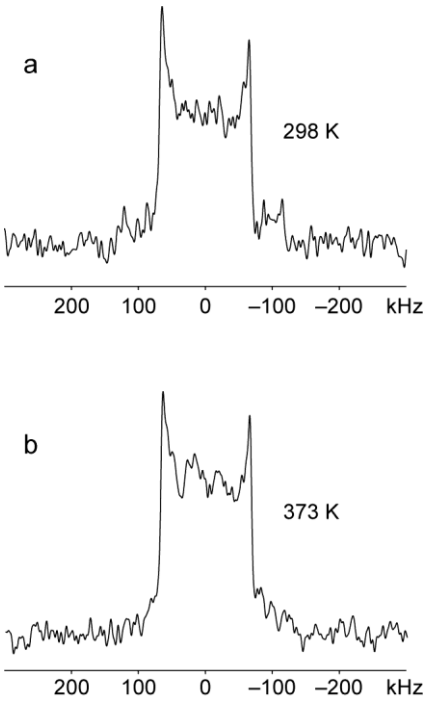

Figure S2.3.1 ^{2}H wideline NMR spectra recorded at temperatures of 298 K (a) and 373 K (b).

Upon closer inspection of the spectrum recorded at 373 K, it is possible that a second, low-intensity pair of 'horns' are present near the centre of the spectrum, although this is almost within the noise level. The close similarity in appearance of both spectra indicates that significant motional processes, such as the flipping of benzene rings that have been observed in MIL-47(V) and MIL-53(Cr),[8] are greatly reduced in MIL-53(Sc). This is consistent with the restricted space available in the narrow channels of the MIL-53(Sc) *cp* structure.

S3. Structural and analytical data for MIL-53(Sc)-NO_2

S3.1 Synthesis, elemental analysis and TGA

Single crystals of MIL-53(Sc)-NO_2 were prepared from a mixture of scandium nitrate hydrate, 2-nitroterephthalic acid, and N,N-diethylformamide (DEF) molar ratio $(Sc(NO_3)_3 \cdot 3H_2O)$:H_2BDC:DEF of 1:1:200. This was stirred at room temperature, transferred to a Teflon-lined stainless-steel autoclave and heated at 463 K for 40 hours. Samples were filtered, washed with ethanol and dried at 313 K. The MIL-53(Sc)-NO_2 crystals were kept under air to obtain a structure for the as-synthesised material. TGA analysis on the ethanol- washed and subsequently vacuum-dried sample showed structural decomposition at 575 – 700 K under flowing air.

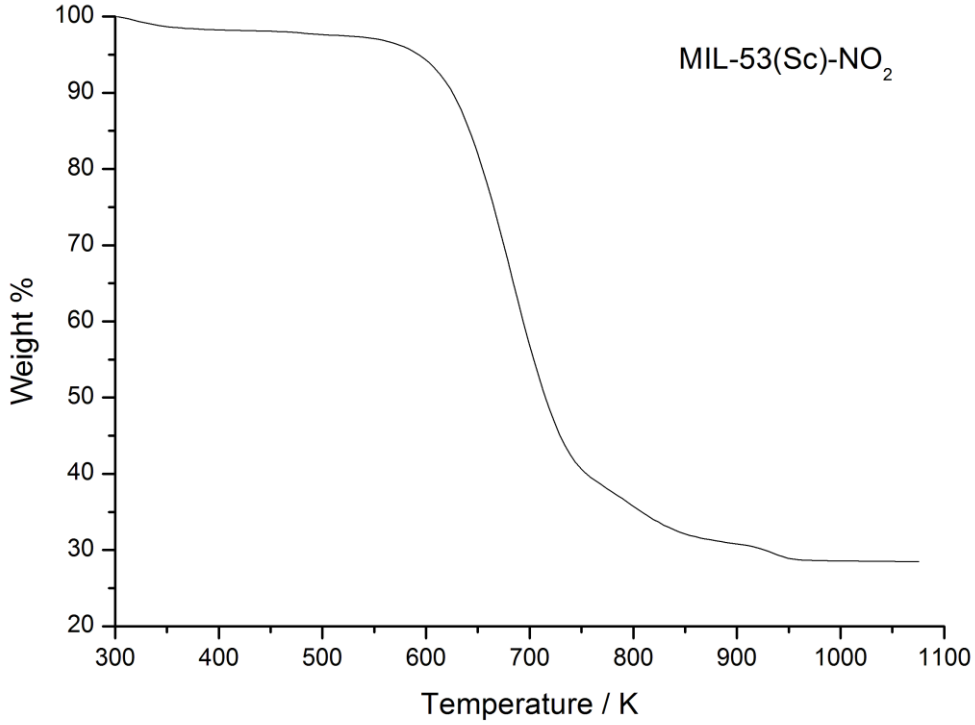

Figure S3.1.1 Thermogravimetric analysis of MIL-53(Sc)-NO_2 shows the material to be stable to heating up to temperatures >550 K under air.

Elemental analysis on the as-prepared material shows reasonable agreement with the calculated values for the MIL-53(Sc)-NO_2 structure, C expected 35.40 wt.%; C measured, 37.62 wt.%, N expected, 5.17 wt.%; N measured, 5.09 wt.% and H expected 1.5 wt.%; measured, 2.3 wt.% although the higher than expected H contents and C:N ratio suggests some residual solvent or water within the channels.

S3.2 ^{45}Sc and ^{13}C solid-state NMR data

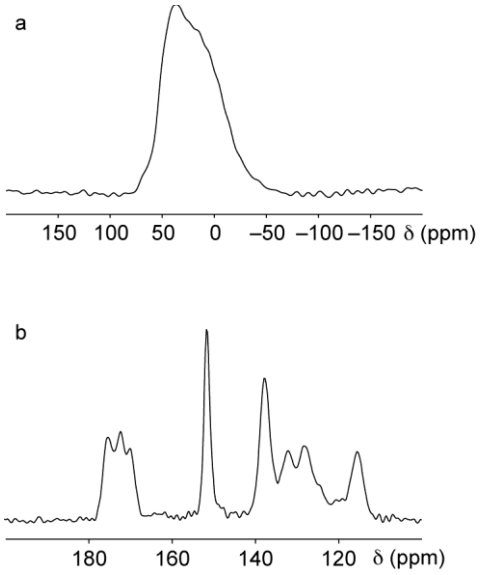

Figure S3.2.1 (a) ^{45}Sc MAS NMR and (b) ^{13}C CPMAS NMR spectra of NO_2-functionalised MIL-53(Sc) recorded at magnetic field strengths of (a) 14.1 T and (b) 9.4 T, and MAS rates of (a) 60 kHz and (b) 12.5 kHz. Spectra are the result of co-adding (a) 384 and (b) 6144 transients, separated by recycle intervals of (a) 1 s and (b) 3 s.

^{13}C and ^{45}Sc spectra of NO_2-functionalised MIL-53(Sc) are shown in Figure S3.2.1 The ^{13}C spectrum confirms the presence of a NO_2 group on the aromatic ring, with a peak observed at δ = 151.7 ppm, corresponding to an aromatic carbon attached to N. The increase in the number of resonances (and their frequency spread) indicates a disorder in the exact position of substitution and lowering of the symmetry. The presence of disorder can also be observed in the ^{45}Sc MAS NMR spectrum, where the features of the quadrupolar lineshape appear broadened.

S3.3 Single-crystal diffraction details

Single crystal diffraction data for MIL-53(Sc)-NO_2 prepared by washing and oven-drying the as-crystallised solid were collected at 293 K on a Rigaku MM007 High brilliance RA generator (Mo K_α radiation, confocal optics) and Mercury CCD system. At least a full hemisphere of data was collected using ω scans. Intensities were corrected for Lorentz-polarisation and for absorption. The structures were solved by direct methods and

structural refinements were performed with full-matrix least-squares based on F^2 by using the program WinGX.[9] In the structure there is one crystallographic carbon atom to which the $-NO_2$ group could be attached. Direct-methods structure solution suggested that there was a $-NO_2$ group present and the site-occupancy was fixed at 0.25 to represent the –NO2 group disordered over the 4 possible positions when symmetry operations are applied. The high displacement factors are attributed to the presence of positional disorder, and additional scattering was refined as O atoms.

Table S3.3.1 Crystallographic data for MIL-53(Sc)-NO_2 from single-crystal X-ray diffraction data.

	MIL-53(Sc)-NO_2
Formula Unit	$ScOH(C_8H_3NO_6)$
Formula Weight	283.05
Temperature/K	93
Space Group	*I* mma
X-ray Source	Mo K_α
Wavelength/Å	0.71075
Unit Cell: *a*/Å	18.279(7)
b/Å	7.330(3)
c/Å	11.601(4)
Volume/ Å^3	1554.4(10)
Z	4
R	0.0778
wR	0.2135
Max and min residual e- density (e/Å^3)	0.726, -0.741

The asymmetric unit of MIL-53(Sc)-NO_2 is given in Table S3.3.2 and shown in Figure S3.3.1 and selected bond distances and ScO_6 octahedron angle are given in Tables S3.3.3 and S3.3.4.

Table S3.3.2 Fractional coordinates, occupancies and displacement factors for MIL-53(Sc)-NO_2

Atom	x	y	z	Occupancy	U (iso or equivalent)
Sc1	0.5	0	0.5	1.0	0.0185(6)
O1	0.5	-0.25	0.5820(4)	1.0	0.0271(12)
O2	0.58196(14)	0.0984(3)	0.6108(3)	1.0	0.0414(9)
C1	0.6099(3)	0.25	0.6338(5)	1.0	0.0379(14)
C2	0.6827(3)	0.25	0.6946(6)	1.0	0.0472(18)
C3	0.7160(3)	0.4090(6)	0.7236(7)	1.0	0.091(3)
N1	0.6904(14)	0.578(4)	0.691(2)	0.25	0.092(7)
O3A	0.7096(13)	0.578(4)	0.691(2)	0.25	0.138(9)
O3B	0.6503(16)	0.641(4)	0.779(2)	0.25	0.150(9)
OW1	0.5	0.75	0.825(3)	0.25	0.155(11)
OW2	0.565(2)	0.75	0.813(3)	0.25	0.115(10)

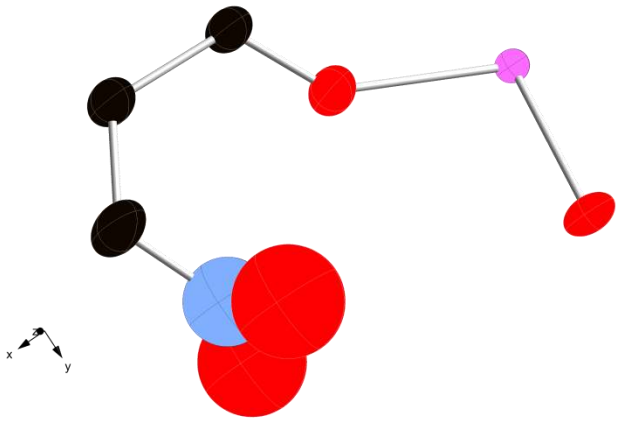

Figure S3.3.1 Asymmetric unit of MIL-53(Sc)-NO_2

Table 3.3.3 Selected bond distances in MIL-53(Sc)-NO_2

Bond	Bond length / Å
Sc1 - O1	2.065(2)
Sc1 - O2	2.102(3)
C1 - O2	1.252(3)
C1 – C2	1.507(8)
C2 – C3	1.357(6)
C3 – N1	1.38(3)
N1 – O3A	1.34(3)
N1 – O3B	1.34(3)

Table S3.3.4 Octahedral bond angles for MIL-53(Sc)-NO_2

Atom 1	Atom 2	Atom 3	Angle / °
O1	Sc1	O1	180.00
O1	Sc1	O2	91.32(11)
O1	Sc1	O2	88.68(11)
O2	Sc1	O2	180.00
O2	Sc1	O2	89.05(17)
O2	Sc1	O2	90.95(17)

The framework structure of MIL-53(Sc)-NO_2 is shown in Figure S3.3.2, viewed down the channel axis. Scattering in the channels was refined as disordered solvent O atoms. The structure has orthorhombic *I mma* symmetry, with a unit cell volume of 1554.4(10) $Å^3$. The -NO_2 group adopts a geometry where the O-N-O plane is perpendicular to the plane of the terephthalate molecule in the framework. This torsion is known for aromatic compounds with a nitro group adjacent to carboxylate and other bulky species.[10,11]

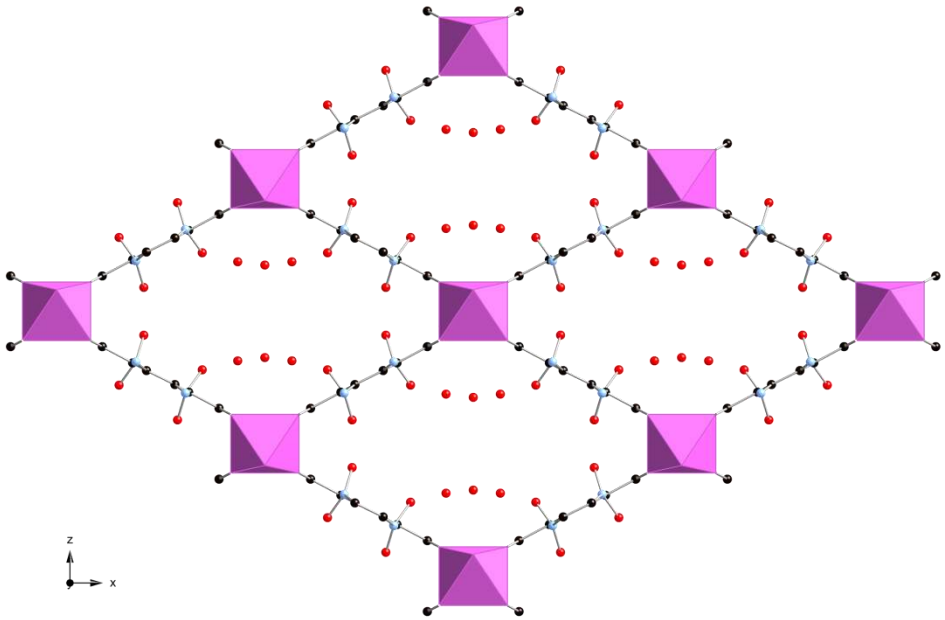

Figure S3.3.2 Structure of the MIL-53(Sc)-NO_2 from single crystal data on the as-prepared sample viewed down the channels. (ScO_6 octahedra in purple, C black spheres; N, blue; O, red)

S3.4 Assessing the structural feasibility of a closed phase for MIL-53(Sc)-NO_2

Synchrotron powder diffraction data of the desolvated, dehydrated form of MIL-53(Sc)-NO_2 has also been collected, and is compared with powder diffraction data on MIL-53(Sc)-*cp* in Figure 3.4.1. The structure retains crystallinity upon dehydration, but it has not yet been possible to solve the structure of dehydrated MIL-53(Sc)-NO_2 .

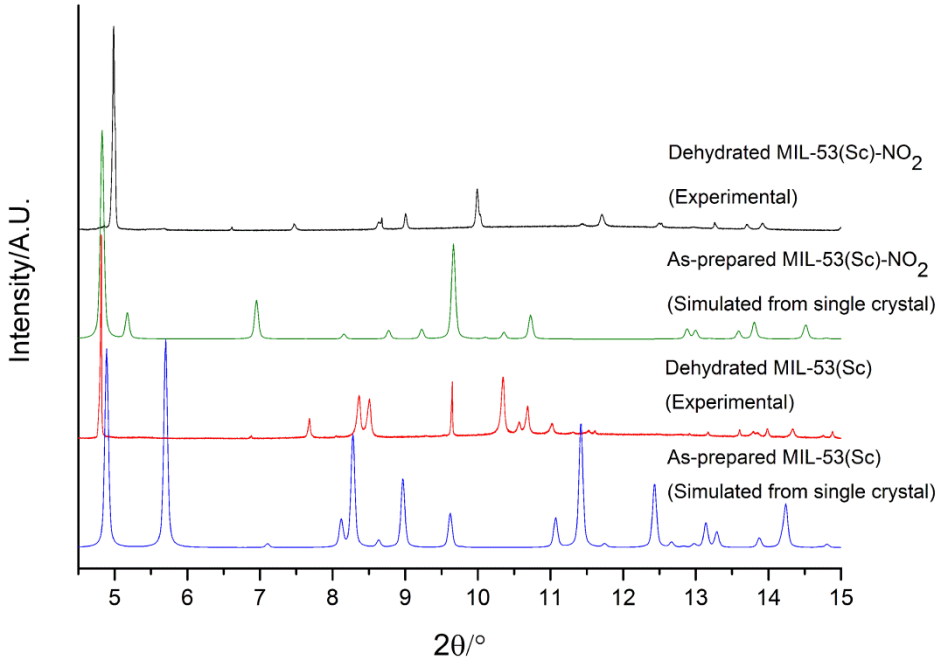

Figure S3.4.1 Synchrotron powder X-ray diffraction data on the MIL-53(Sc) and MIL-53(Sc)-NO_2 in the dehydrated forms compared to simulated patterns of the as-synthesised structures from single crystal data.

To assess the possibility that the nitro form might close, NO_2 groups were placed geometrically on terephthalate rings in the crystal structure of MIL-53(Sc)-*cp* at 298 K. The non-bonding distances from the oxygen atoms of the hypothetical $–NO_2$ groups to aromatic carbon atoms of neighbouring terephthalate groups were found to be in the range 1.33 – 2.74 Å. These close distances of approach would not be possible (the sum of the van der Waals radii of O and N is greater than 3 Å), indicating that the NO_2-functionalised structure must remain partially open upon removal of all guest molecules from the channels.

S4. Adsorption data

Samples that had already been heated in the tube furnace to remove guest molecules were heated to 473 K *in vacuo* for an additional 12 hours to ensure complete dehydration.

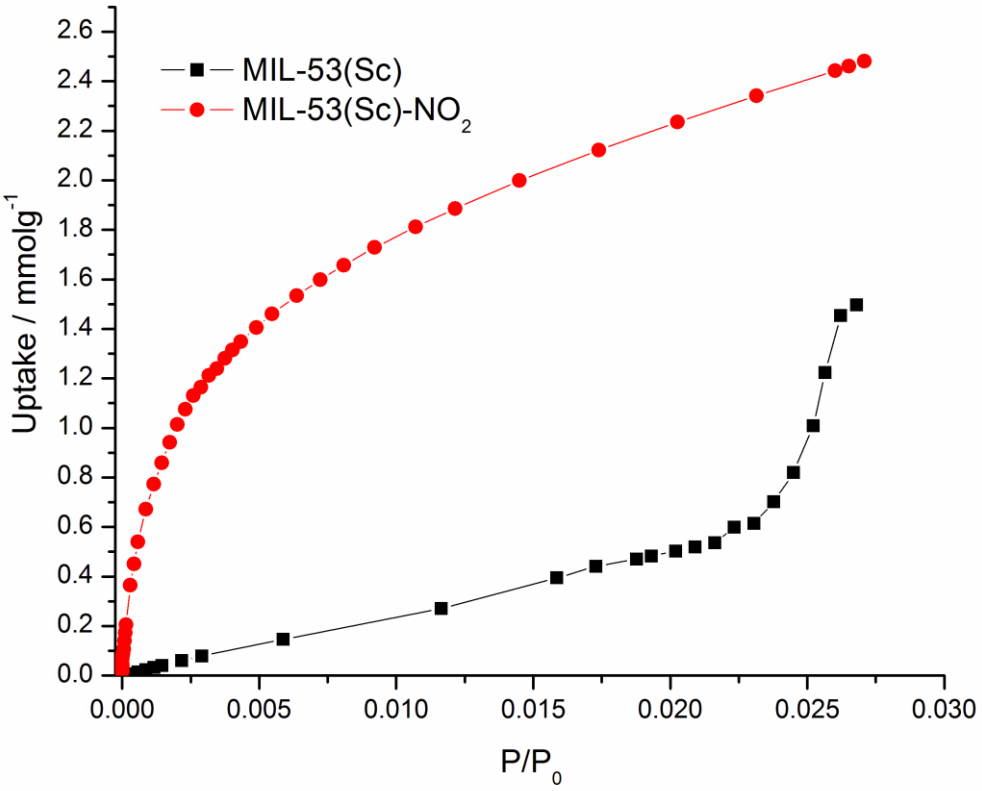

Figure S4.1 CO_2 adsorption isotherms at 273 K. The red circles show the adsorption isotherm of MIL-53(Sc)-NO_2 and the black squares the adsorption MIL-53(Sc).

Adsorption experiments on the MIL-53(Sc) and the –NO_2 functionalised derivative at 273 K *again* show that there is greatly increased uptake in the low pressure region of the isotherm indicating that, as the crystallography suggests, the structure is propped open by the bulky nitro group.

S.5 Computational Simulation of CO_2 Adsorption

CO_2 adsorption on five MIL-53(Sc) structures was investigated using grand canonical Monte Carlo (GCMC) simulation[12] implemented in the multipurpose simulation code Music.[13] These five structures were:

1. MIL-53(Sc)-*cp* (this paper, with H atoms added and the structure optimized using CASTEP[7] with a fixed unit cell obtained from the synchrotron powder refinement)
2. MIL-53(Sc)–*vnp*; (this paper, with H atoms added and the structure optimized using CASTEP[7] with a fixed unit cell obtained from the synchrotron powder refinement)
3. MIL-53(Sc)-H_2O,[1] with water removed (with the H atoms added geometrically using the structure solution from powder refinement as the model)
4. MIL-53(Sc)-DMF,[1] minus dimethylformamide solvent molecules (from the crystal structure with geometrically positioned H atoms)
5. large pore MIL-53(Sc)–*lp*, derived from a model of MIL-53(Cr)-*lp*[14] by replacing Cr^{3+} by Sc^{3+}, followed by geometry optimization using CASTEP[7] (allowing the unit cell to vary).

In the grand canonical ensemble, the chemical potential, the volume and the temperature are kept fixed as in adsorption experiments. Atomistic models were used for the MIL-53(Sc) structures, with the atoms frozen at the crystallographic positions. In the simulations, CO_2 molecules were randomly moved, rotated, inserted and deleted, allowing the number of molecules in the framework to fluctuate. The chemical potential was related to the system pressure by the Peng-Robinson equation of state.[15]

The standard 12-6 Lennard-Jones (LJ) potential was used to model the interatomic interactions. The parameters for the framework atoms were obtained from the Dreiding force field,[16] except for Sc, obtained from UFF,[17] while CO_2 was modeled by the TraPPE three-center model[18] (Table 1). The Lorentz-Berthelot mixing rules were employed to calculate the mixed parameters. Interactions beyond 15 Å were neglected for the simulations. Mulliken partial charges for the framework atoms were calculated using CASTEP[7] and are resumed in Table 1 and Figure 1. The atoms to which the charges were assigned are labeled in Figure 1. A total number of 5×10^7 Monte Carlo steps were performed. The first 40% was used for system equilibration, carefully ensuring that thermodynamic equilibrium was reached, while the remaining steps were used to calculate the ensemble averages.

Pore size distributions (PSD) were calculated with the method developed by Gelb and Gubbins which determines the diameter of the largest sphere that can fit into the cavities without overlapping with any of the framework atoms.[19]

Table S.5.1. Lennard-Jones Parameters and Partial Charges.

	σ [Å]	**ε/kB [K]**	**q [e]**
C (in CO_2)	2.800	27.000	0.66
O (in CO_2)	3.050	79.000	-0.33
Sc1	2.936	9.561	1.67
C1	3.473	47.856	-0.06
C2	3.473	47.856	-0.24
O1	3.033	48.158	-0.89
O2	3.033	48.158	-0.60
H1	2.846	7.649	0.42
H2	2.846	7.649	0.28

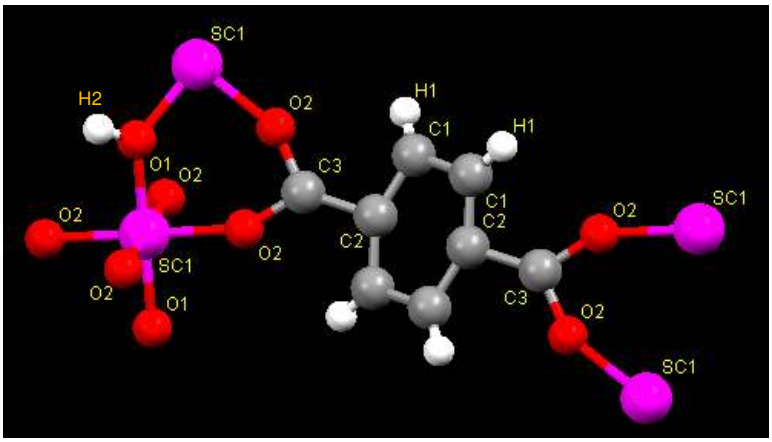

Figure S.5.1: MIL-53(Sc)-open with atoms labelled corresponding to the partial charges assigned: oxygen, hydrogen, carbon, and scandium are marked in red, light grey, dark grey, and brown.

Simulated isotherms are given in figure S.5.2. No adsorption was predicted for the intermediate structure, MIL-53(Sc)-H_2O (shown) or the very narrow pore structure, MIL-53(Sc)–*vnp* (not shown), for which the pore sizes are too small (< 2.5 Å). The adsorption of the as-prepared structure, MIL-53(Sc)-DMF (minus the dimethylformamide molecules

present in the experimental structure) is larger than that observed in the first step (see also figure S.5.2), indicating the structure does not open to that extent. The maximum uptake predicted for the large pore structure is close to that observed above 80 kPa (CO_2).

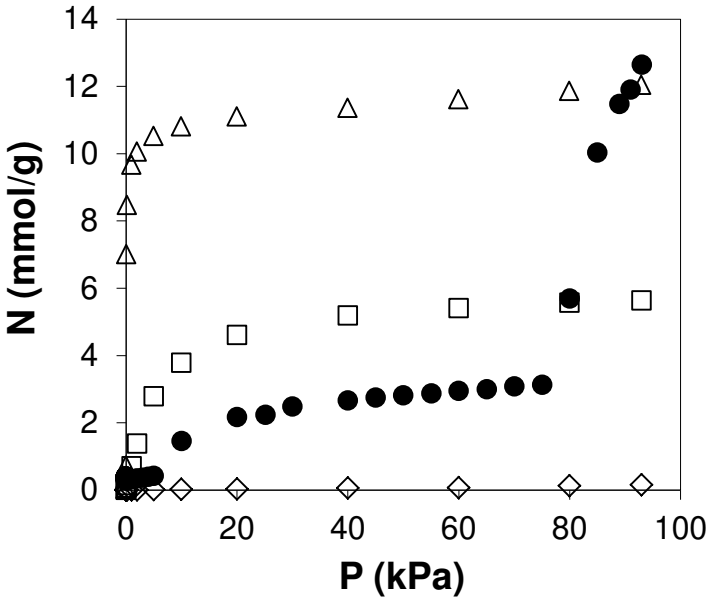

Figure S5.2. Predicted CO_2 adsorption isotherm on MIL-53(Sc) at 196 K: experimental, full circles; and simulated data on as-prepared structure, MIL-53(Sc)-DMF, open squares; intermediate structure, MIL-53(Sc)-int, from MIL-53(Sc)-H_2O, open rhombus; and large-pore structure, MIL-53(Sc)-lp, open triangles. No adsorption was predicted for the very narrow pore structure.

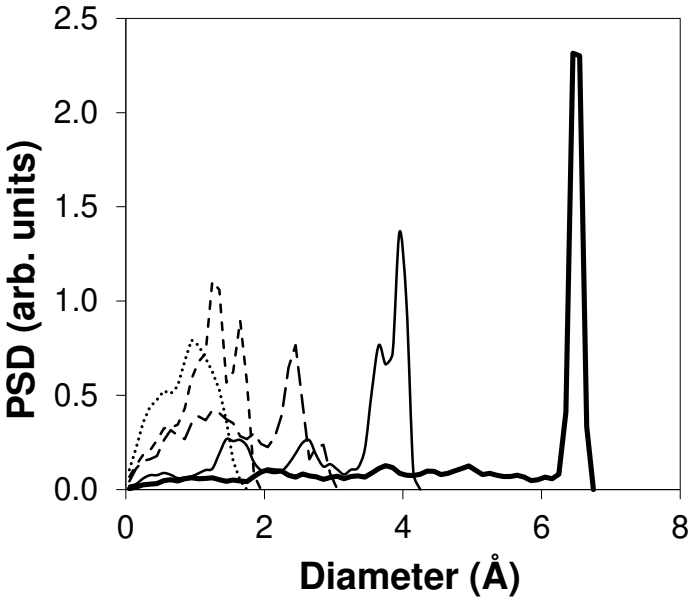

Figure S.5.3. Pore size distributions of MIL-53(Sc) structures: MIL-53(Sc)-cp, dotted line; MIL-53(Sc)-vnp, dashed line; MIL-53(Sc)-int, long dashed line; MIL-53(Sc)-DMF, solid line; and MIL-53(Sc)-lp, bold solid line.

S6. References

1. J. P. S. Mowat, S. R. Miller, A. M. Z. Slawin, V. R. Seymour, S. E. Ashbrook and P. A. Wright, *Micropor. Mesosopor. Mat.* 2011, **142**, 322.
2. G. M. Sheldrick, *Acta Cryst. A*, 2008, **64**, 112.
3. S. P. Brown and S. Wimperis, *J. Mag. Res*. 1997, **124**, 279.
4. K. J. Pike, R. P. Malde, S. E. Ashbrook, J. McManus and S. Wimperis, *Solid State Nucl. Magn. Reson.* 2000, **16**, 203.
5. S. Antonijevic and S. Wimperis, *J. Magn. Reson*. 2003, **164**, 343.
6. S. J. Clark, M. D. Segall, C. J. Pickard, P. J. Hasnip, M. J. Probert, K. Refson and M. C. Payne, *Zeit. Krist*., 2005, **220**, 567.
7. C. J. Pickard and F. Mauri, *Phys. Rev. B*, 2001, 63.
8. D. I. Kolokolov, H. Jobic, A. G. Stepanov, M. Plazanet, M. Zbiri, J. Ollivier, V. Guillerm, T. Devic, C. Serre and G. Férey, Eur. Phys. *J.-Sp. Top*. 2010, **189**, 263.
9. L. J. Farrugia, *J. Appl. Cryst*. 1999, **32**, 837.
10. S. J. Grabowski and T. M. Krygowski, *Acta. Cryst. C*, 1985, **41**, 1224.
11. D. J. A. Deridder and H. Schenk, *Acta. Cryst. B*, 1995, **51**, 221.
12. D. Frenkel and B. Smit, *Understanding Molecular Simulations: From Algorithms to Applications*. 2nd Ed.; Academic Press: San Diego, 2002.
13. A. Gupta, S. Chempath, M. J. Sanborn, L. A. Clark and R. Q. Snurr, *Molecular Simulation* 2003, **29**, 29.
14. C. Serre, F. Millange, C. Thouvenot, M. Nogues, G. Marsolier, D. Louer and G. Férey, . *J. Am. Chem. Soc,* 2002, **124**, 13519
15 (a) D.-Y. Peng and D. B. Robinson, *Ind. Eng. Chem., Fundam*. 1976, **15**, 59. (b) R. C. Reid, J. M. Pausnit and B. E. Poling, *The Properties of Gases and Liquids*, 4th Ed., McGraw-Hill Companies (NY), 1987.
16. S. L. Mayo, B. D. Olafson and W. A. Goddard, Dreiding, *J. Phys. Chem*., 1990, **94**, 8897.
17. A. K. Rappé, C. J. Casewit, K. S. Colwell, W. A. Goddard and W. M. Skiff, *J. Am. Chem. Soc.* 1992, **114**, 10024.
18. J. J. Potoff and J. I. Siepmann, *AIChE Journal*, 2001, **47**, 1676.
19. L. D. Gelb and K. E. Gubbins, *Langmuir* 1999, **15**, 305.